Absorption with Instantaneous Reaction in a Droplet with Sparingly Soluble Fines

Fabrizio Scala
Istituto di Ricerche sulla Combustione, C.N.R., 80125 Napoli, Italy

Michele D'Ascenzo
Dipt. di Ingegneria Chimica, Università degli Studi di Napoli Federico II, 80125 Napoli, Italy

The problem of gas absorption followed by an instantaneous irreversible chemical reaction in a rigid droplet containing sparingly soluble fine reactant particles is discussed. A model was developed for the general case when the reactant particle dissolution near the gas–liquid interface is nonnegligible. Solids dissolution is treated taking into account the average spacing between the suspended particles. A simple analytical expression for the rate of gas absorption is derived under the assumption of slow particle dissolution, and conditions are given for applicability of the model. A numerical example, relevant for the spray-dry desulfurization process, for the system SO_2-$Ca(OH)_2$ in water is discussed.

Introduction

The absorption of a gas into a slurry, followed by a chemical reaction between the dissolved gas and a solute dissolving from the sparingly soluble fine particles is of great practical relevance in the chemical industry. One example is found in gas purification processes, where the suspended solid particles provide a continuous supply of reactant in order to enhance the gas absorption rate. Particularly important is the case when the chemical reaction between the dissolved reactants can be considered instantaneous and irreversible. The absorption of sulfur dioxide into a lime slurry is an example of a widely used application of this case. A typical way of bringing the gaseous stream into contact with the slurry is to disperse the liquid phase into droplets in order to increase the gas–liquid interface area, as in spray-dry desulfurization.

Ramachandran and Sharma (1969) were the first to theoretically discuss the problem of gas absorption with chemical reaction and with sparingly soluble fine particles, and they proposed two film models, depending on whether solid dissolution in the liquid film was important or not. Analytical solutions were derived and results showed that the gas absorption rate could be considerably enhanced by the presence of solids. Uchida et al. (1975) extended the analysis to account for the increase of solid dissolution in the liquid film due to the chemical reaction. Uchida et al. (1977) considered the case when the concentration of reactant dissolving from the particles in the bulk liquid phase is lower than the saturation solubility (slow dissolution rate compared to gas absorption rate). Uchida and Wen (1977) classified the problem of gas absorption into a slurry into six categories according to the reactant concentration profiles that are formed in the liquid phase. For each case a model was given based on film theory and an analytical solution provided. Based on their own experimental results, Sada et al. (1984) further modified the theory in order to account for the presence of an inert region without particles near the gas–liquid interface. Yagi and Hikita (1987) criticized the previous models, pointing out that a parameter representing the average interparticle spacing is necessary to characterize the system and that it is inappropriate to use a mass-transfer coefficient for particle dissolution. Recently Mehra (1996) examined the process of particle dissolution near the gas–liquid interface and pointed out that the change in particle size should be accounted for when the particles are small enough for significant dissolution. He also criticized the approach of Sada et al. (1984), indicating that there is no physical reason why a particle-free zone should exist near the gas–liquid interface. In his article, he proposed a penetration model based on a transient population balance near the gas–liquid interface that was solved numerically for some representative cases.

Correspondence concerning this article should be addressed to F. Scala.

All the references reported so far refer to planar geometry. Partridge et al. (1990) presented a mechanistic model of sulfur dioxide absorption into a lime slurry in a spray dryer, where the solution of Ramachandran and Sharma (1969) for the case of negligible solid dissolution in the liquid film was simply combined with an existing mathematical description of the spray-dry operation. To simulate gas absorption into a slurry droplet, however, a more detailed model is needed. Few extensions of the problem to spherical geometry have been reported in the literature. Newton et al. (1990) presented a model of sulfur dioxide absorption into a lime slurry droplet in a spray dryer, where solids circulation within the droplet was assumed to be negligible. Mass-transfer processes within the droplet and around the suspended particles were examined in detail and a complex trial-and-error procedure was used to solve the model equations. Recently, Mungistein et al. (2001) developed a model for gas absorption into a large slurry droplet, that took internal circulation inside the droplet into consideration. The model, relevant to spray towers, was solved numerically, and results indicated that for large droplets internal circulation enhances the mass transfer with respect to a stagnant droplet.

In this work the problem of gas absorption followed by an instantaneous irreversible chemical reaction into a rigid droplet containing sparingly soluble fine reactant particles is considered, assuming slow reactant particle dissolution. This assumption implies that particle shrinkage is negligible, so that a constant particle size can be assumed. A model is developed for the general case when the reactant particle dissolution near the gas–liquid interface is nonnegligible. Solids dissolution is treated in a rigorous way, and the average spacing between the suspended particles is taken into account. A simple analytical expression is provided for the gas absorption rate. A numerical example, relevant to the spray-dry desulfurization process, for the SO_2-$Ca(OH)_2$ system in water is discussed.

Theory

The problem can be represented by the following scheme

$$A(\mathrm{g}) \rightarrow A(\mathrm{aq})$$
$$B(\mathrm{s}) \rightarrow B(\mathrm{aq})$$
$$A(\mathrm{aq}) + B(\mathrm{aq}) \rightarrow \text{products} \qquad (1)$$

The theoretical treatment is based on the following simplifying assumptions:

1. Both gaseous and solid reactants have low solubility in the liquid;
2. Reaction between the two species is instantaneous and irreversible;
3. The influence of product species on the process is negligible;
4. Solid particle dissolution is slow, so particle shrinkage can be neglected;
5. Solid particles are spherical, uniform in size, uniformly dispersed in the liquid phase, and do not agglomerate;
6. There is no surface kinetic resistance to particle dissolution, which is entirely controlled by mass transfer;
7. Solid particles are stationary (nondiffusing) and the liquid around the particles can be considered stagnant, as discussed by Mehra (1996);
8. The droplet is spherical and rigid, and water and sorbent particles do not circulate within the droplet. This assumption is based on the consideration that typical droplet sizes encountered in the spray-dry process are of the order of 10–100 μm. It has been reported that no internal circulation occurs for this small size (Newton et al., 1990; Hill and Zank, 2000).
9. Heats of reaction and dissolution are small and can be neglected, and the system is isothermal.

The system is shown in Figure 1. A sharp "macroscopic" spherical reaction front concentric to the gas–liquid interface occurs at the steady state at a distance λ from the droplet center, where reactant concentration falls to zero. This reaction front divides the droplet (of radius R_D) into two zones. In the zone between the interface and the reaction front ($\lambda < R < R_D$), only reactant A exists in the liquid phase. Due to the presence of the dissolving solid particles, a small microscopic spherical reaction front occurs around each particle in this zone, as shown in Figure 2a. Beyond the macroscopic reaction front ($0 < R < \lambda$), only reactant B exists in the liquid phase. Around each dissolving particle in this zone a gradient of reactant B occurs, as shown in Figure 2b.

If r_P is the solid particles radius and ϵ_P is the solids volume fraction in the slurry, the number of particles per unit volume of slurry is

$$N = \frac{3\epsilon_P}{4\pi r_P^3} \qquad (2)$$

It is thought that the unit slurry volume can be divided into N nonoverlapping cells (assumed spherical), with a solid particle at their center. Each particle has a volume of slurry in its cell equal to $1/N$. The radius of each cell is

$$r_C = \frac{r_P}{\sqrt[3]{\epsilon_P}} \qquad (3)$$

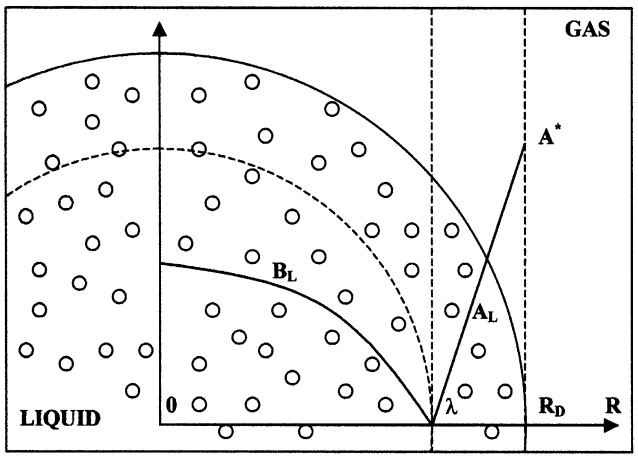

Figure 1. Gas absorption with instantaneous reaction in a rigid slurry droplet.

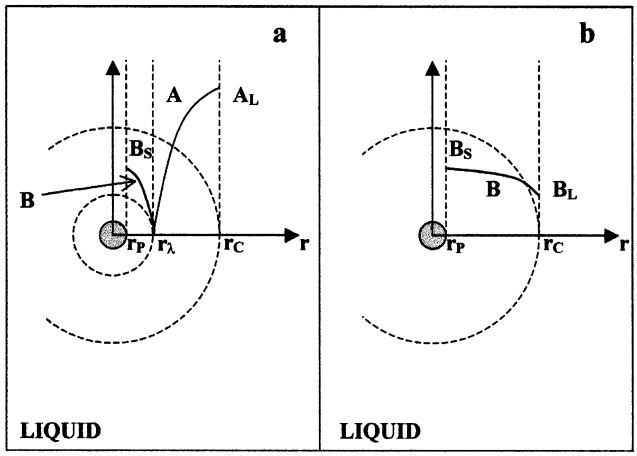

Figure 2. Reactants concentration profiles around one fine particle.

(a) Particles between gas–liquid interface and the macroscopic reaction front. (b) Particles beyond the macroscopic reaction front.

Let us now consider the particles present in the zone between the gas–liquid interface and the macroscopic reaction front ($\lambda < R < R_D$) (Figure 2a). The concentration of B at the surface of the particles is at the equilibrium with the solid (saturation solubility), namely B_S. On the other hand, at the external cell surface, the concentration of reactant A is as in the liquid phase, namely A_L. Somewhere between the particle surface and the cell surface ($r_P < r < r_C$), a microscopic reaction front occurs, at a distance r_λ from the particle center, where reactant concentration falls to zero. This reaction front divides the spherical cell into two zones: a zone near the particle surface where only reactant B is present ($r_P < r < r_\lambda$), and a zone near the external cell surface, where only reactant A is present ($r_\lambda < r < r_C$). The material balances in the two zones give

$$\frac{d}{dr}\left(r^2\frac{dB}{dr}\right)=0 \quad \begin{cases} r=r_P \Rightarrow B=B_s \\ r=r_\lambda \Rightarrow B=0 \end{cases} \tag{4}$$

$$\frac{d}{dr}\left(r^2\frac{dA}{dr}\right)=0 \quad \begin{cases} r=r_\lambda \Rightarrow A=0 \\ r=r_C \Rightarrow A=A_L \end{cases} \tag{5}$$

The solutions of the two equations are, respectively

$$B=B_S\left(\frac{r_\lambda/r-1}{r_\lambda/r_P-1}\right) \tag{6}$$

$$A=A_L\left(\frac{1-r_\lambda/r}{1-r_\lambda/r_C}\right) \tag{7}$$

At the reaction front the fluxes of the two reactants must equal each other

$$D_B\left.\frac{dB}{dr}\right|_{r_\lambda} = -D_A\left.\frac{dA}{dr}\right|_{r_\lambda} \tag{8}$$

Equation 8 allows the calculation of r_λ

$$r_\lambda = r_P\left[\frac{1+\dfrac{D_B B_S}{D_A A_L}}{1+\dfrac{r_P}{r_C}\left(\dfrac{D_B B_S}{D_A A_L}\right)}\right] \tag{9}$$

The flux of reactant A per unit external surface of the cell is

$$-D_A\left.\frac{dA}{dr}\right|_{r_C}=\frac{D_A A_L + D_B B_S}{r_C(r_C/r_P-1)} \tag{10}$$

The consumption of reactant A per unit volume of slurry is given by

$$G_A = 3\frac{D_A A_L + D_B B_S}{r_C^2(r_C/r_P-1)} = (1-\epsilon_P)\alpha^2(D_A A_L + D_B B_S)/R_D^2 \tag{11}$$

where (using Eq. 3)

$$\alpha = \frac{R_D}{r_C}\sqrt{\frac{3}{(1-\epsilon_P)(r_C/r_P-1)}} = \frac{R_D}{r_P}\sqrt{\frac{3\epsilon_P}{(1-\epsilon_P)\left(1-\sqrt[3]{\epsilon_P}\right)}} \tag{12}$$

Let us now shift attention to the particles suspended in the zone inside the macroscopic reaction front ($0 < R < \lambda$) (Figure 2b). No reactant A is present in this zone. At the surface of the particles the concentration of reactant B is B_S, while at the external cell surface, it is equal to that in the liquid phase, namely B_L. The material balance on reactant B in the cell gives

$$\frac{d}{dr}\left(r^2\frac{dB}{dr}\right)=0 \quad \begin{cases} r=r_P \Rightarrow B=B_S \\ r=r_C \Rightarrow B=B_L \end{cases} \tag{13}$$

The solution is

$$B=B_S\left(\frac{r_C/r-1}{r_C/r_P-1}\right)+B_L\left(\frac{1-r_P/r}{1-r_P/r_C}\right) \tag{14}$$

The flux of reactant B per unit external surface of the cell is

$$-D_B\left.\frac{dB}{dr}\right|_{r_C}=-\frac{D_B(B_S-B_L)}{r_C(r_C/r_P-1)} \tag{15}$$

The generation of reactant B per unit volume of slurry is given by

$$G_B=-3\frac{D_B(B_S-B_L)}{r_C^2(r_C/r_P-1)}=-(1-\epsilon_P)\alpha^2 D_B(B_S-B_L)/R_D^2 \tag{16}$$

At this point, the material balances in the droplet liquid phase before and after the macroscopic reaction front can be carried out with reference to Figure 1 (using Eqs. 11 and 16), are

$$(1-\epsilon_P)\frac{D_A}{R^2}\frac{d}{dR}\left(R^2\frac{dA_L}{dR}\right)=G_A=(1-\epsilon_P)\alpha^2 \times(D_A A_L+D_B B_S)/R_D^2 \quad \begin{cases} x=\lambda \Rightarrow A_L=0 \\ x=R_D \Rightarrow A_L=A^* \end{cases} \tag{17}$$

$$(1-\epsilon_P)\frac{D_B}{R^2}\frac{d}{dR}\left(R^2\frac{dB_L}{dR}\right)=G_B=-(1-\epsilon_P)\alpha^2 D_B \times(B_S-B_L)/R_D^2 \quad \begin{cases} x=0 \Rightarrow dB_L/dR=0 \\ x=\lambda \Rightarrow B_L=0 \end{cases} \tag{18}$$

where the term $(1-\epsilon_P)$ on the lefthand side (LHS) accounts for the reduced volume for diffusion due to the presence of the solid particles. Let us make the following change of variables

$$\vartheta_A=1+\frac{D_A A_L}{D_B B_S} \tag{19}$$

$$\vartheta_B=(B_S-B_L)/B_S \tag{20}$$

If we define $\eta=R/R_D$, Eqs. 17 and 18 become

$$\frac{d}{d\eta}\left(\eta^2\frac{d\vartheta_A}{d\eta}\right)=\alpha^2\eta^2\vartheta_A \quad \begin{cases} \eta=\eta_\lambda \Rightarrow \vartheta_A=1 \\ \eta=1 \Rightarrow \vartheta_A=\vartheta^* \end{cases} \tag{21}$$

$$\frac{d}{d\eta}\left(\eta^2\frac{d\vartheta_B}{d\eta}\right)=\alpha^2\eta^2\vartheta_B \quad \begin{cases} \eta=0 \Rightarrow d\vartheta_B/d\eta=0 \\ \eta=\eta_\lambda \Rightarrow \vartheta_B=1 \end{cases} \tag{22}$$

where $\eta_\lambda=\lambda/R_D$ and

$$\vartheta^*=1+\frac{D_A A^*}{D_B B_S} \tag{23}$$

Noting that the boundary condition at the reaction front

$$D_B\frac{dB_L}{dR}\bigg|_\lambda=-D_A\frac{dA_L}{dR}\bigg|_\lambda \tag{24}$$

implies the identity

$$\frac{d\vartheta_A}{d\eta}\bigg|_{\eta_\lambda}=\frac{d\vartheta_B}{d\eta}\bigg|_{\eta_\lambda} \tag{25}$$

the problem can be simplified by solving the single equation

$$\frac{d}{d\eta}\left(\eta^2\frac{d\vartheta}{d\eta}\right)=\alpha^2\eta^2\vartheta \quad \begin{cases} \eta=0 \Rightarrow d\vartheta/d\eta=0 \\ \eta=1 \Rightarrow \vartheta=\vartheta^* \end{cases} \tag{26}$$

The solution of Eq. 26 reads

$$\vartheta=\vartheta^*\frac{\sinh(\alpha\eta)}{\sinh(\alpha)\eta} \tag{27}$$

where $\vartheta=\vartheta_A$ for $1<\vartheta<\vartheta^*$ and $\vartheta=\vartheta_B$ for $0<\vartheta<1$. Location of the macroscopic reaction front along the droplet radius can be found by imposing $\vartheta=1$ when $\eta=\eta_\lambda$ in Eq. 27. The gas absorption rate per unit interface area is

$$J_A^*=-(1-\epsilon_P)D_A\frac{dA_L}{dR}\bigg|_{R_D}=\frac{\beta}{R_D}(D_A A^*+D_B B_S)=\frac{\beta}{R_D}D_A A^*\left(1+\frac{D_B B_S}{D_A A^*}\right) \tag{28}$$

where

$$\beta=(1-\epsilon_P)\left(\frac{\alpha}{\tanh(\alpha)}-1\right) \tag{29}$$

Equation 28 is very easy to handle; for example, if Henry's law is assumed to hold at the interface ($p^*=HA^*$), Eq. 28 can be combined with the gas-phase diffusion resistance to give

$$J_A^*=\frac{D_A p_G/H+D_B B_S}{R_D/\beta+D_A/(k_G H)} \tag{30}$$

where p_G is the bulk-gas partial pressure of reactant A, and k_G is the gas-side mass-transfer coefficient. The bulk gas is supposed to be perfectly mixed.

The treatment so far has been based on the assumption that a macroscopic reaction front occurs inside the droplet, somewhere between the droplet center and the gas–liquid interface (Figure 1). Should the solids dissolution be very slow compared to the gas absorption, the macroscopic reaction front would be able to reach the droplet center. This would happen if

$$\vartheta^*\geq\frac{\sinh(\alpha)}{\alpha} \tag{31}$$

In this case no macroscopic reaction front occurs at the steady state, and only reactant A exists in the liquid phase in the whole droplet. A microscopic reaction front is found around each dissolving solid particle (as shown in Figure 2a). Also Eqs. 26–30 are able to handle this case, the only difference being that in the solution (Eq. 27) $\vartheta=\vartheta_A>1$ always would be along the droplet radius. Combining Eq. 31 with Eq. 28 and considering the gas-phase diffusion resistance, the condition for this case occurring results

$$p_G\geq D_B B_S\left[\left(\frac{H}{D_A}+\frac{\beta}{k_G R_D}\right)\frac{\sinh(\alpha)}{\alpha}-\frac{H}{D_A}\right] \tag{32}$$

It is interesting to study the asymptotic behaviors: if $H\rightarrow\infty$, or if the following condition is satisfied

$$p_G\leq\beta D_B B_S/k_G R_D \tag{33}$$

the surface concentration of reactant A goes to zero, the reaction front shifts to the gas–liquid interface ($\lambda=R_D$) and the absorption rate is entirely controlled by gas-phase resistance (reactant B is assumed to be nonvolatile), that is

$$J_A^*=k_G p_G \tag{34}$$

This also would be the case when $r_P\rightarrow 0$, but in that case the initial assumption that solid-particle dissolution is slow would

not be valid and particle shrinkage could not be neglected. On the other hand, for a very dilute suspension ($\epsilon_P \to 0$) no steady-state solution can be found. The physical reason for this is that solid particles are unable to provide a continuous supply of reactant B to the liquid phase.

Conditions for applicability of the model

We now discuss how limited the model is as regards to the size of the suspended reactant particles. The condition is determined by the initial assumption that particle dissolution is slow, so that particle shrinkage can be neglected. One way to estimate the time interval in which this condition holds is as follows. Using Eq. 10 to calculate the maximum rate of dissolution of one particle, we get

$$G_{P,\max} = -4\pi r_C^2 D_A \left.\frac{dA}{dr}\right|_{r_C,\max} = 4\pi \frac{D_A A^* + D_B B_S}{(1/r_P - 1/r_C)} \quad (35)$$

The particle volume change per unit time is given by

$$\frac{\Delta V_P}{\Delta t} = \frac{M}{\rho_P} G_{p,\max} = \frac{M}{\rho_P} 4\pi \frac{D_A A^* + D_B B_S}{(1/r_P - 1/r_C)} \quad (36)$$

where M is the molecular weight, and ρ_P is the particle density. Making the fractional volume change lower than a certain value: $\Delta V_P/V_P < \xi$. This implies that (using Eq. 3)

$$\Delta t < \xi \left(\frac{\rho_P}{3M} \frac{r_P^3 (1/r_P - 1/r_C)}{D_A A^* + D_B B_S} \right) = \xi \left(\frac{\rho_P}{3M} \frac{r_P^2 \left(1 - \sqrt[3]{\epsilon_P}\right)}{D_A A^* + D_B B_S} \right) \quad (37)$$

Equation 37, thus, sets the time interval for the applicability of the model.

One last consideration should be added. From Yagi and Hikita's (1987) discussion, one could point out that the concentration profiles around the dissolving solid particles and those in the droplet liquid phase overlap, which causes a distortion in the profiles. While for very low solids volume fractions, the solid particles have a very low effect on the process, Eq. 9 indicates that for large solids volume fractions the microscopic reaction front nearly coincides with the particle surface. This implies that the mathematical development reported in this work could be used to treat the whole range of solids volume fractions of interest.

Numerical Example

As a representative case, we chose the absorption of SO_2 (reactant A) into an aqueous slurry droplet of $Ca(OH)_2$ (reactant B) at ambient conditions. This example is relevant to spray-dry desulfurization processes. The ionic reaction in the liquid phase between the two dissolved reactants can be considered irreversible and instantaneous (Babu et al., 1984). The physical-parameter values for this system have been estimated as follows

$$D_A = 1.8\times10^{-9}\ \text{m}^2/\text{s}$$
$$D_B = 1.6\times10^{-9}\ \text{m}^2/\text{s}$$
$$B_S = 2.0\times10^{-2}\ \text{kmol}/\text{m}^3$$
$$H = 7.3\times10^{-1}\ \text{atm}\cdot\text{m}^3/\text{kmol}$$
$$M = 74\ \text{kg}/\text{kmol}$$
$$\rho_P = 2.2\times10^{3}\ \text{kg}/\text{m}^3$$

In order to evaluate the gas-side mass-transfer coefficient, the droplet is assumed to flow at its terminal velocity. This would set the most conservative conditions. For 10–100-μm-size droplets, terminal velocities are always more than one order of magnitude lower than typical flue-gas velocities, so it is reasonable to assume that the droplet travels at the same velocity as the flue gas (no slip velocity). As a consequence, it is assumed that the droplet Sherwood number (Sh) is equal to the limiting theoretical value of 2 relative to the stagnant boundary-layer condition. The gas-side mass-transfer coefficient is then given by

$$k_G = \frac{D_G Sh}{2R_D \Re T} = \frac{D_G}{R_D \Re T} \quad (38)$$

where $\Re$ is the gas-law constant, and T is the system temperature. The sulfur dioxide diffusion coefficient in the gas phase is estimated to be $D_G = 1.4\times10^{-5}\ \text{m}^2/\text{s}$.

The first step is to establish the conditions for the applicability of the model. The typical range of particle sizes in the slurry used in practice is $1\ \mu\text{m} < r_P < 10\ \mu\text{m}$. According to Eq. 37 for this particle-size range (a value of $\xi = 0.1$ was used), the model would be applicable approximately for $\Delta t < 0.01 - 0.1$ s. At this point, it is interesting to examine the specific features of the system SO_2-$Ca(OH)_2$ slurry. As will be shown later, for all the operating conditions of practical interest, the macroscopic reaction front is very close to the droplet surface, as the solids dissolution rate is very fast with respect to the gas absorption rate. As a consequence, the solid particles near the gas–liquid interface are bound to be dissolved much more rapidly than the others, so that after a relatively short time a particle-free zone would be created near the droplet surface. On the other hand, in a typical spray-dry operation, water evaporates from the droplets, whose surface recedes as the droplet decreases in size. This process tends to compensate particle depletion near the droplet surface, so the model developed here is likely to be applicable to the whole droplet lifetime. Of course, for a detailed simulation of the process, the droplet-size decrease and the particle-number depletion, as well as the solids volume fraction, increase with time should be taken into account by combining the absorption model with a detailed spray-dry reactor model. In any event, even simple considerations using the equations developed so far lead to quite interesting results, as is shown in the following.

Figures 3 and 4 show the condition in Eq. 33 for the particle- and droplet-size ranges of interest at three different solids volume fraction. The area below the curves represents the range of sulfur dioxide partial pressures in the gas phase for which the gas absorption is completely controlled by gas-side

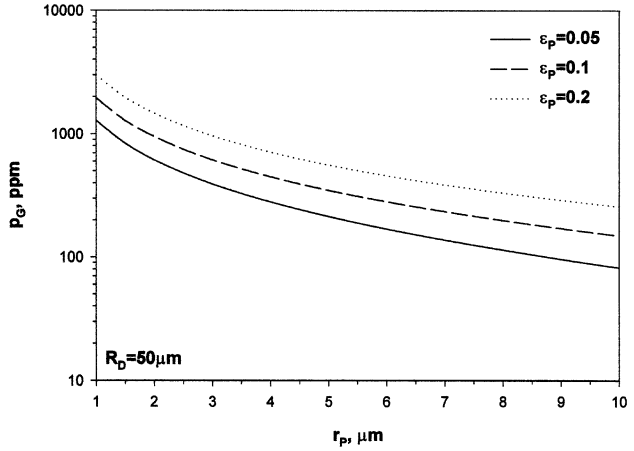

Figure 3. Condition in Eq. 33 for the particle-size range of interest at three different slurry solids volume fractions.

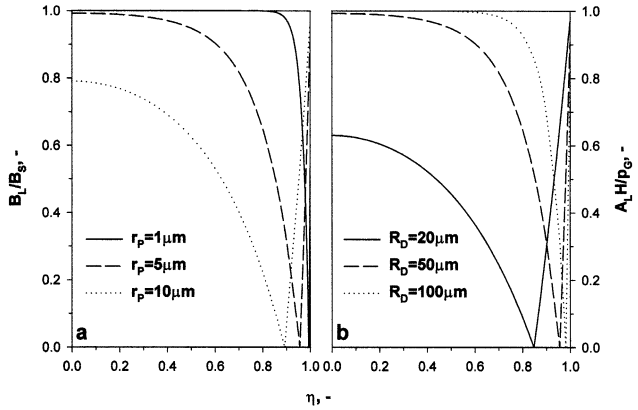

Figure 5. Reactant concentration profiles in the droplet (a) for three different particle sizes at $R_D = 50$ μm; (b) for three different droplet sizes at $r_P = 5$ μm: $\epsilon_P = 0.1$; $p_G = 5{,}000$ ppm.

diffusion resistance, that is, Eq. 34 holds. It is clearly seen that for most flue-gas purification processes, both the gas- and liquid-side resistances are relevant. In particular, for low sulfur dioxide partial-pressure, gas-side resistance controls the absorption process, while for high partial pressures, liquid-side resistance controls the process. Analysis of the order of magnitude of the two terms in the denominator in the RHS of Eq. 30 shows that for most practical operating conditions, liquid- and gas-side resistances have the same magnitude. Decreasing the size of the suspended particles (Figure 3) and increasing the solids volume fraction or the droplet size (Figure 4) enhances the relevance of the gas-side resistance to the absorption process.

On the other hand, the condition in Eq. 32 would be satisfied only for sulfur dioxide partial pressures in a gas phase well above one atmosphere for all operating conditions of interest. So in practical conditions the macroscopic reaction front never reaches the droplet center, but always stays close to the gas–liquid interface.

Figures 5 and 6 report the reactant concentration profiles in the droplet for three particle sizes (Figure 5a), for three droplet sizes (Figure 5b), for three solids volume fractions (Figure 6a), and for three gas sulfur dioxide partial pressures (Figure 6b). In the figures the reactant concentrations have been normalized, respectively, with the calcium hydroxide saturation solubility and with the sulfur dioxide concentration that would be in equilibrium with the actual gas partial pressure (p_G/H). Sulfur dioxide partial pressure values are all above the curves reported in Figures 3 and 4. It can be clearly seen that, as a consequence of rapid particle dissolution, the reaction front is always close to the droplet surface. The reaction front approaches the gas–liquid interface as the particle size and the SO_2 concentration decrease or as the droplet size and solids volume fraction increase.

Figure 7 depicts the gas absorption rate per unit interface area as a function of the SO_2 partial pressure for three different particle sizes. For comparison, the maximum gas ab-

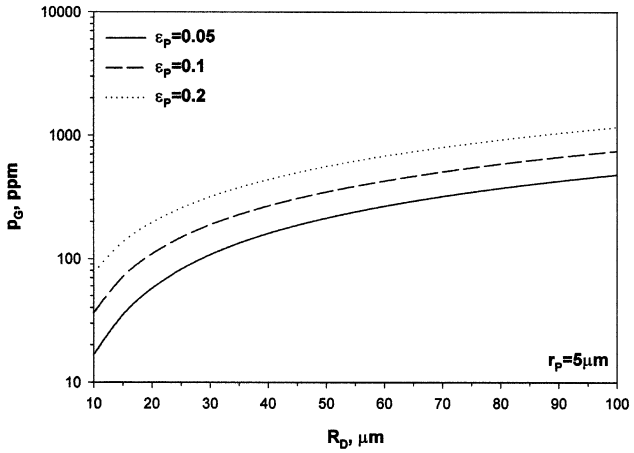

Figure 4. Condition in Eq. 33 for the droplet-size range of interest at three different slurry solids volume fractions.

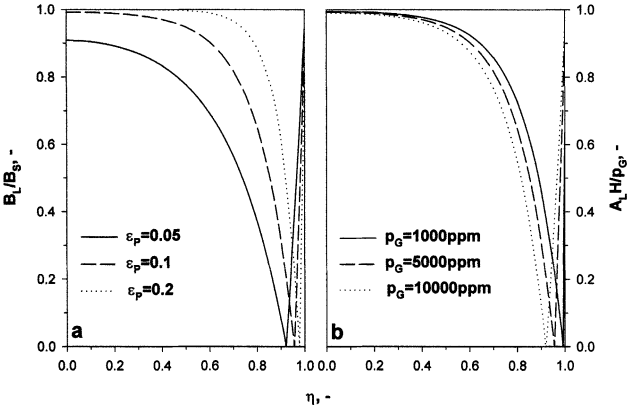

Figure 6. Reactant concentration profiles in the droplet (a) for three different solids volume fractions at $p_G = 5{,}000$ ppm; (b) for three different SO_2 partial pressures at $\epsilon_p = 0.1$: $r_P = 5$ μm; $R_D = 50$ μm.

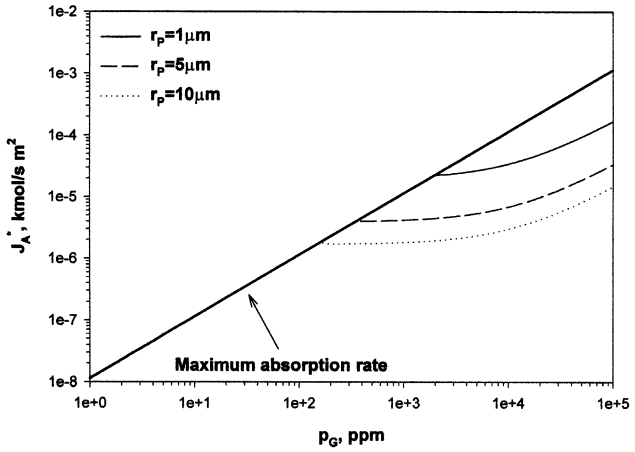

Figure 7. Sulfur dioxide absorption rate per unit interface area as a function of SO_2 bulk gas partial pressure for three different particle sizes: $R_D = 50$ μm; $\epsilon_P = 0.1$.

sorption rate (that is, complete gas-side control; Eq. 34) is also shown. Analysis of the figure shows that, while at low SO_2 partial pressures, the absorption rate is the maximum possible, at relatively high partial pressures, the curves tend toward lower values. In particular, the larger the particle size, the lower the gas absorption rate. Figure 8 shows the influence of the droplet size and the solids volume fraction on the gas absorption rate per unit interface area, for a SO_2 gas partial pressure of $p_G = 5{,}000$ ppm. Both these variables exert a limited influence, as the gas absorption rate is slightly larger when the droplet size and solids volume fraction are increasing.

On the whole, the model results suggest that at low SO_2 partial pressures the absorption rate is controlled by gas-side resistance. In these conditions, the only way to enhance the absorption rate is to increase the mass-transfer coefficient, for example, by reducing the droplet size. On the other hand, at high SO_2 partial pressures liquid-side resistance controls

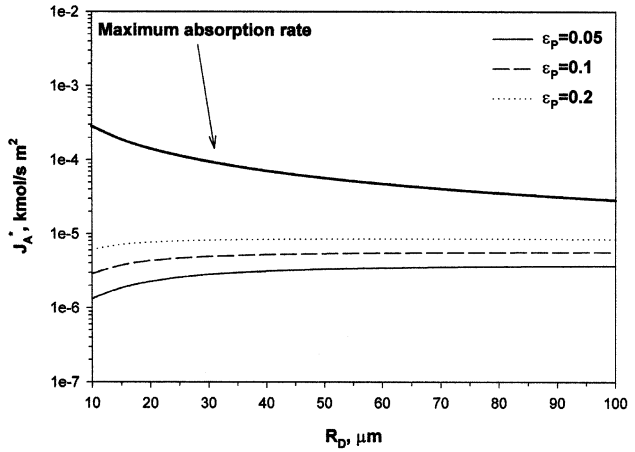

Figure 8. Sulfur dioxide absorption rate per unit interface area as a function of droplet size for three different solids volume fractions: $r_P = 5$ μm; $p_G = 5{,}000$ ppm.

the absorption rate. In these conditions, the absorption rate can be enhanced by decreasing the suspended particle size and to a lesser extent by increasing the droplet size and solids volume fraction. Solids dissolution is always very rapid and would give an appreciable resistance to the absorption rate only at SO_2 partial pressures well above those typically encountered in flue-gas purification processes.

When analyzing the reported results, however, it must be borne in mind that optimization of the operating variables in a practical operation is much more complex and must take into account a number of other factors, such as droplet trajectory, residence time in the reactor, exposed interface area, heat transfer, evaporation, spray-nozzle characteristics, possible solids recycle, and lime slaking.

Conclusions

The problem of gas absorption followed by an instantaneous irreversible chemical reaction in a rigid droplet containing sparingly soluble fine reactant particles has been considered. This problem has considerable industrial importance, for example, in gas purification processes. A model has been developed for the general case when reactant particle dissolution is nonnegligible next to the gas–liquid interface. Solids dissolution is treated in a rigorous way of accounting for the average spacing between the particles in the slurry. A simple analytical expression for the rate of gas absorption is derived, assuming slow particle dissolution. The time interval for which the model is applicable is determined.

A numerical example for SO_2 absorption into an aqueous slurry droplet of $Ca(OH)_2$ at ambient conditions is presented and discussed. This example is relevant for the spray-dry desulfurization process. Results show that for most practical operating conditions, the gas absorption rate is controlled by a combination of gas- and liquid-side diffusion resistances. Solids dissolution is always very rapid and exerts negligible resistance to the absorption process. The gas absorption rate can be enhanced by using a smaller particle size, and to a lesser extent by increasing the solids volume fraction and the droplet size. On the other hand, at low SO_2 partial pressures the only way to enhance SO_2 absorption is to increase the gas-side mass-transfer coefficient.

Acknowledgments

Useful discussion with Prof. A. Lancia is gratefully acknowledged.

Notation

A = liquid concentration of reactant A, kmol/m^3
A^* = interface liquid concentration of reactant A, kmol/m^3
a = gas–liquid interface area per unit volume of liquid, m^{-1}
B = liquid concentration of reactant B, kmol/m^3
D = diffusion coefficient, m^2/s
G = consumption (generation) rate per unit volume of slurry, kmol/m^{3}s
$G_{P,\max}$ = maximum dissolution rate of one particle, kmol/s
H = Henry's constant, atm m^3/kmol
J^* = gas absorption rate per unit interface area, kmol/m^{2}s
k_G = gas-side mass-transfer coefficient, kmol/m^{2}atm s
M = molecular weight, kg/kmol
N = number of particles per unit volume of slurry, m^{-3}
p = partial pressure, atm
$\Re$ = gas-law constant, atm m^3/kmol K
R = radial coordinate in the droplet, m
r = radial coordinate around suspended particles, m

Sh = Sherwood number
T = system temperature, K
t = time, s
V = volume, m^3

Greek letters

α = coefficient defined in Eq. 12
β = coefficient defined in Eq. 29
ϵ = volume fraction
η = dimensional radial coordinate in the droplet ($= R/R_D$)
λ = macroscopic reaction front distance from the droplet center, m
ρ = density, kg/m^3
ϑ = variable defined in Eqs. 19 and 20
ϑ^* = interface value of ϑ defined in Eq. 23
ξ = coefficient in Eq. 37

Subscripts

A = reactant A
B = reactant B
C = cell
D = droplet
G = gas phase
L = liquid phase
P = solid particle
S = saturation
λ = reaction front

Literature Cited

Babu, D. R., G. Narsimhan, and C. R. Phillips, "Absorption of Sulfur Dioxide in Calcium Hydroxide Solutions," *Ind. Eng. Chem. Fundam.*, **23**, 370 (1984).

Hill, F. F., and J. Zank, "Flue Gas Desulphurization by Spray Dry Absorption," *Chem. Eng. Process*, **39**, 45 (2000).

Mehra, A., "Gas Absorption in Reactive Slurries: Particle Dissolution Near Gas-Liquid Interface," *Chem. Eng. Sci.*, **51**, 461 (1996).

Munginstein, A., M. Fichman, and C. Gutfinger, "Gas Absorption in a Moving Drop Containing Suspended Solids," *Int. J. Multiphase Flow*, **27**, 1079 (2001).

Newton, G. H., J. Kramlich, and R. Payne, "Modeling the SO_2-Slurry Droplet Reaction," *AIChE J.*, **36**, 1865 (1990).

Partridge, G. P., W. T. Davis, R. M. Counce, and G. D. Reed, "A Mechanistically Based Model of Sulfur Dioxide Absorption into a Calcium Hydroxide Slurry in a Spray Dryer," *Chem. Eng. Commun.*, **96**, 97 (1990).

Ramachandran, P. A., and M. M. Sharma, "Absorption with Fast Reaction in a Slurry Containing Sparingly Soluble Fine Particles," *Chem. Eng. Sci.*, **24**, 1681 (1969).

Sada, E., H. Kumazawa, and C. H. Lee, "Chemical Absorption into Concentrated Slurry—Absorptions of Carbon Dioxide and Sulfur Dioxide into Aqueous Concentrated Slurries of Calcium Hydroxide," *Chem. Eng. Sci.*, **39**, 117 (1984).

Uchida, S., K. Koide, and M. Shindo, "Gas Absorption with Fast Reaction into a Slurry Containing Fine Particles," *Chem. Eng. Sci.*, **30**, 644 (1975).

Uchida, S., K. Koide, and C. Y. Wen, "Gas Absorption with Fast Reaction into a Slurry: Case of Fast Gas Absorption Rate Compared with Solid Dissolution Rate," *Chem. Eng. Sci.*, **32**, 447 (1977).

Uchida, S., and C. Y. Wen, "Rate of Gas Absorption into a Slurry Accompanied by Instantaneous Reaction," *Chem. Eng. Sci.*, **32**, 1277 (1977).

Yagi, H., and H. Hikita, "Gas Absorption into a Slurry Accompanied by Chemical Reaction with Solute from Sparingly Soluble Particles," *Chem. Eng. J.*, **36**, 169 (1987).

Manuscript received Sept. 7, 2001, and revision received Jan. 28, 2002.